



# Trajectory Planning of Quadrotor UAV with Maximum Payload and Minimum Oscillation of Suspended Load Using Optimal Control

Danial Hashemi<sup>1</sup> · Hamidreza Heidari<sup>1</sup>

Received: 7 December 2018 / Accepted: 30 January 2020 / Published online: 10 March 2020  
© Springer Nature B.V. 2020

## Abstract

This paper focuses on the problem of transporting a cable-suspended load by a quadrotor UAV for safer flight and more efficiency. The dynamic model of a quadrotor coupled to the suspended load is derived using the Euler-Lagrange formulation. The optimal trajectory for carrying the maximum payload and minimum oscillation of swinging load will be obtained. The optimal cable length to increase the maximum payload capacity and reduce the maximum oscillation angle of swinging load is obtained. Also, the effect of load mass on the maximum oscillation angle of swinging load is studied. In this paper, the optimization procedure is based on the solution of the optimal control problem from the class of open loop with an indirect method. The application Pontryagin's Minimum Principle lead to deriving the optimality conditions and subsequently a two-point boundary value problem (TPBVP) which is solved by a numerical method. An appropriate algorithm is presented for calculating the maximum payload to move between two specified points. The main superiority of this method is that it can solve a wide range of optimal maneuvers for arbitrary initial and final configurations relevant to every considered cost function. Generating various optimal paths with different maximum payloads and oscillation angles by modifying the values of the penalty matrices. In order to verify the efficiency of the proposed method and the presented algorithm, a simulation study is performed for a quadrotor with a suspended load in maneuver between two specified points and various object function.

**Keywords** Quadrotor · Maximum payload · Minimum swing · Optimal control · Path planning · Suspended load

## 1 Introduction

Quadrotors are multirotor helicopters which are known as unmanned aerial vehicles (UAV). Many unique abilities like hover, take off, fly and land vertically in small areas making them capable of performing various military and civilian operations. Photography, inspection, research platform, relief operations, fly in high-risk areas, cargo transportation and in various other similar applications. Among the various applications of quadrotors, in recent years, aerial load transportation has attracted the attention of craftsmen more than before. This feature has a vast range of applications such as sending first-aid kits to the sufferers in natural mishaps like earthquakes, fires, floods, industrial accidents, as well as transportation of cargo which is carried out by some shipping companies and some stores. Finding the optimal path for quadrotor

can have a significant effect on more productivity and safer flight. Trajectory planning is a special case of the general motion planning problem, which is a complex task to solve, especially when the number of degrees of freedom is large. A quadrotor with an inelastic cable-suspended load in the three-dimensional space has eight degrees of freedom, and it has differential constraints including limited speed and maximum acceleration. Therefore, in this paper, the indirect solution of the open loop optimal control problem is used for the optimization procedure. Optimal control is a powerful procedure which can be employed in both classes open-loop and closed-loop. The closed-loop optimal control based on the linear quadratic regulator is extensively employed in manipulator robots as a state feedback control [1]. But, in the open-loop optimal control method due to the off-line quiddity despite the closed loop, many problems such as system nonlinearities and all kinds of constraints can be considered. In other words, the open-loop optimal control method based on Pontryagin's Minimum Principle (PMP) is an appropriate method is in cases where the system has a large number of degrees of freedom or where optimizing the different objectives is desired [2].

✉ Hamidreza Heidari  
hr.heidari@malayeru.ac.ir

<sup>1</sup> Department of Mechanical Engineering, Malayer University, Malayer, Iran

The purpose of trajectory planning is to move the quadrotor from the original location to the desired location by defining the rotor velocities of the quadrotor. Design and analyzing of optimization process are commonly begun by regarding mathematical models of physical systems. The model of a system is so important because it gives how to move the system, forces involved and how the system responds to inputs given to it. A proper dynamic system modeling must include a faithful mathematical description of the whole system. The basic dynamical model of quadrotor is the starting point for all of the studies, but more sophisticated aerodynamic properties were have been introduced as well [3, 4]. Luukkonen derived the differential equations of a quadrotor from both the Euler-Lagrange equations and the Newton-Euler equations which are both used in the study of quadrotors [5]. Bousbaine et al. focused their research on the modeling of small size quadrotor helicopters. They developed a detailed dynamic analytical model of the quad-rotor helicopter using the linear Taylor series approximation method. The model is further calibrated and linearized for use on any quad-rotor helicopter [6]. With introduction of inexpensive micro-Unmanned Aerial Vehicles (MAV) and development of the technology of these robots, such as creating precision controllers and sophisticated sensors, controllers have been designed for many tasks like aggressive maneuvers [7], balancing a flying inverted pendulum [8], dynamic trajectory generation [9] and also this progressions leads very well to using UAVs for transportation of external loads. M. Guerrero et al. derived the dynamic model of a quadrotor system with a cable-suspended load using Euler-Lagrange formulation in which the integrated dynamics of the system include quadrotor, cable, and payload was considered. They also developed an Interconnection and Damping Assignment-Passivity Based Control (IDA-PBC) for the system to carry the payload between two points with reducing the oscillation along the path [10]. Since a quadrotor is inherently unstable, adding a suspended load to the quadrotor, exacerbates instability. Therefore, the problem of stability and propose a robust control strategy also, canceling or reducing oscillation of the suspended load based on anti-swing control has been a concern for several researchers [11–14].

On the other hand, obtaining an optimal trajectory for a quadcopter is a hard task due to complex dynamics. Several researchers have also proposed algorithms that find trajectories from a class of motion primitives and respect the dynamic constraints of quadrotors [15–17]. These algorithms compel dynamic feasibility by designing trajectories in a two-step process. First, determine the shape of the trajectory and then determine an appropriate speed profile so that feasibility constraints are not violated. Hehn et al. applied an algorithm that allows the calculation of quadrotor maneuvers that satisfy Pontryagin's Minimum Principle concerning time-optimality for arbitrary initial and final states. Such maneuvers provide a

useful lower bound on the duration of maneuvers, which can be used to assess the performance of controllers and vehicle design parameters [18]. Lai et al. considered a time-optimal movement of the hovering quadrotor helicopter between two configurations. Nonlinear programming (NLP) method is proposed to solve a set of highly nonlinear differential equations. However, since the quadrotor helicopter is a nonlinear system, it will be a difficult task to find a feasible solution for the formulated NLP problem. Therefore, a genetic algorithm was used to generate feasible solutions for the time-optimal problem [19]. For the sake of performance improvement and economic efficiency of robots in the field of transportation of external loads, it is important to find the maximum payload capacity. Hence, in the last two decades, various investigations have been conducted on this. Many previous investigations about this, were based on Iterative Linear Programming (ILP). Ghariblu and Korayem used the ILP procedure to determine the Maximum Allowable Load (MAL) of a flexible mobile manipulator. They presented a proper algorithm to acquire the optimal trajectory for maximum payload through linearizing the dynamic equation and constraints [20]. But when nonlinear terms of the system are high and fluctuating, linearization of dynamical equations in ILP procedure is a difficult task. Wang et al. utilized a different method to calculate the maximum payload for open chained manipulators based on the resolution of the optimal control problem with a direct method [21]. The basis of this strategy is the parameterization of the optimization problem. Then, it uses methods like Particle Swarm Optimization (PSO), genetic algorithm, etc. to solve it. But this method is also feeble, because of limiting the solution to a fixed-order polynomial and also, intricacy issues appeared in differentiating torques.

Heidari and Korayem presented an approach to determine the Maximum Allowable Dynamic Load (MADL) of geometrically nonlinear flexible link mobile manipulators. The optimal procedure was based on a solution of optimal control problem from the class of open loop by an indirect method. Using PMP to this problem lead to a two-point boundary value problem (TPBVP), which is solved by numerical techniques. Also, they developed a path planning algorithm for the solution of the TPBVP to find the maximum payload [22]. The main superiority of this procedure is that through the change in the values of the penalty matrices, various trajectories are found in which different objectives are optimized relative to their importance. Accordingly, the designer can choose the most proper path amidst the various optimal paths.

Among the numerous papers in the field of the trajectory planning of a quadrotor with a swinging, maximum payload capacity is rarely considered. Also, due to the complex dynamics of a quadrotor with a swinging load and a high number of degrees of freedom, the optimization problem is a difficult task. Unlike previous methods, the indirect method does not need to limit the solution to a fixed-order polynomial and

divergence does not happen. The indirect method provides a precise resolution of the optimization problem. The simulation results show the power and efficiency of the method to overcome the high nonlinearity nature of the problem such as path optimization of quadrotors.

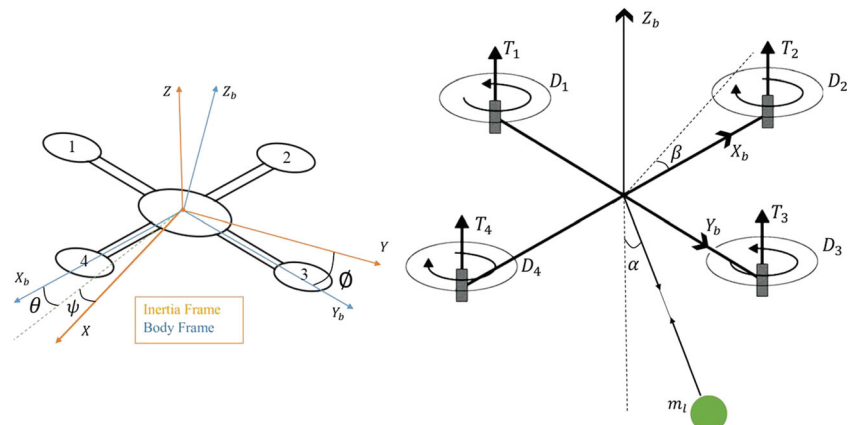
In this paper, the optimal trajectory for carrying the maximum payload and minimum oscillation of suspended load is obtained. The ratio of cable length to quadrotor length for increasing the maximum payload carrying capacity and reducing the maximum oscillation angle of suspended load are calculated. The effect of load mass on the maximum oscillation angle of suspended load is studied. Also, in order to validate the robustness of the proposed control strategy, how the system performs under disturbances are studied. For this purpose, the structure of the system and how it moves is described, and the aerodynamic and Euler-Lagrange equations of the system are obtained. The presented method for solving optimality problem is based on the solution of the open loop optimal control problem with an indirect method which is employed to derive optimality conditions. The Hamiltonian function is formulated according to the objective function. Then based on PMP, the essential conditions for optimality are achieved. The achieved conditions lead to a TPBVP which is solved by a collocation method with the BVP4C command in MATLAB®. In order to obtain the maximum allowable load and its corresponding optimal path, a computational algorithm is developed. Finally, to confirm the effectiveness and importance of the proposed method, some simulations for a quadrotor with a cable-suspended load are performed, and the results are discussed.

## 2 Dynamics Modeling

### 2.1 System Structure

A quadrotor system with a cable-suspended load which has eight degrees of freedom is shown in Fig. 1. Firstly,

**Fig. 1** Schematic view of a quadrotor system



to describe how the system moves, two coordinate systems are introduced. The Inertial-Frame which is also called the global coordinate system represents a right-hand inertia frame with the  $z$ -axis being the vertical direction to the earth and everything discussed can be referenced. The Body-Frame that is attached to the mass center of the quadrotor and it is often used to simplify relationships.

Quadrotors have four rotors that provide the force required for linear motion of the center of mass in directions  $x$ ,  $y$ ,  $z$ , and rotation around the mass center by the spin of their blades. The various movements of the quadrotor are caused by changes in the angular velocity of rotors. As shown in Fig. 1, the direction of rotating adjacent rotors is opposite to each other to avoid rotation around the  $z$ -axis continuously. In order to move in the direction of the  $z$ -axis requires that the speed of each of the four rotors increase or decrease with the same values. If the speed of rotor 1 (or 2) increases and the speed of rotor 3 (or 4) decreases, then the roll ( $\phi$ ) (or pitch ( $\theta$ )) motion is created. Also, if the speed of the rotors 1 and 3 increase to the same value and the speed of the rotors 2 and 4 is also decrease to the same value as 1 and 3, then the Yaw ( $\psi$ ) motion is created [23, 24]. Assuming the cable length  $r$  is constant,  $\gamma$ ,  $\beta$  shows the angular position of mass relative to the quadrotor. Therefore, the configuration variables of the system in the I-F are as follows.

$$q = [x \ y \ z \ \psi \ \theta \ \phi \ \alpha \ \beta]^T \in \mathbb{R}^{8 \times 1} \quad (1)$$

In which  $\xi = [x \ y \ z]^T$  and  $\eta = [\psi \ \theta \ \phi]^T$  denote the position and attitude of the quadrotor in I-F, respectively. And  $\mu = [\alpha \ \beta]^T$  shows the suspended load angle.

### 2.2 Aerodynamic Equations of Rotor and Propeller

The resultant forces applied to the blades of the propeller create a force and a torque in the  $z$ -axis direction, which are respectively called Thrust Force and Drag torque, based on the

theory of blade elements [25] their values for rotor "i" is calculated as follows.

$$\begin{aligned} T_i &= b\omega_i^2, & D_i &= d\omega_i^2 \\ b &= C_T \frac{4\rho R^4}{\pi^2}, & d &= C_D \frac{4\rho R^5}{\pi^3} \end{aligned} \quad (2)$$

In which  $C_T$  and  $C_D$  are the thrust and drag factor respectively,  $\rho$  is the air density and  $R$  is the propeller radius.

By collecting thrust force and drag torque of four rotors and assuming  $C_T$  and  $C_D$  is identical for each rotor, the whole system's thrust and drag in B-F are obtained as follows.

$$\begin{aligned} F_t &= \sum_{i=1}^4 T_i = b \sum_{i=1}^4 \omega_i^2, \\ F_b &= \begin{bmatrix} 0 \\ 0 \\ F_t \end{bmatrix}, \quad \tau_b = \begin{bmatrix} \tau_\phi \\ \tau_\psi \end{bmatrix} = \begin{bmatrix} lb(-\omega_2^2 + \omega_4^2) \\ lb(-\omega_3^2 + \omega_1^2) \\ d \sum_{i=1}^4 (-1)^i \omega_i^2 \end{bmatrix} \end{aligned} \quad (3)$$

The summary form of system inputs for the optimal control problem is defined as follows.

$$\begin{aligned} U_1 &= T_1 + T_2 + T_3 + T_4 \\ U_2 &= U_\phi = l(T_4 - T_2) \\ U_3 &= U_\theta = l(T_3 - T_1) \\ U_4 &= U_\psi = (-D_1 + D_2 - D_3 + D_4) \end{aligned} \quad (4)$$

In which  $l$  is the distance of two rotors opposite to each other.

## 2.3 Euler-Lagrange Equations

The following assumptions are considered for modeling the quadrotor with a swinging load.

- 1) The cable mass and aerodynamic effects of the payload are ignored.
- 2) The payload can be considered as a mass point.
- 3) The cable is considered to be inelastic, and its length is constant.
- 4) Thrust factor and Drag factor of each propeller are the same.

$$b_1 = b_2 = b_3 = b_4, \quad d_1 = d_2 = d_3 = d_4$$

- 5) Mass distribution of the quadrotor is symmetrical in the  $x$ - $y$  plane.
- 6) Both bodies are assumed to be rigid.

Kinetic and potential energies of the system for the Lagrangian formulation are obtained. The whole system potential energy  $K(q, \dot{q})$  stems from the translational and

rotational movement of the system. And it can be expressed as a sum of two functions the kinetic energy of quadrotor [10].

$$K_q = \frac{1}{2} M \dot{\xi}^T \dot{\xi} + \frac{1}{2} \dot{\eta}^T J \dot{\eta} \quad (5)$$

And the kinetic energy of swinging load.

$$K_l = \frac{1}{2} m_l \dot{x}_l^2 + \frac{1}{2} m_l \dot{y}_l^2 + \frac{1}{2} m_l \dot{z}_l^2 + \frac{1}{2} I (\dot{\alpha}^2 + \dot{\beta}^2) \quad (6)$$

$M$  and  $m_l$  are the values of the quadrotor mass and the payload, respectively.  $I_\psi$ ,  $I_\theta$  and  $I_\phi$  denote the moments of inertia of the quadrotor and  $I$  is the moment of inertia of the payload. The coordinates of the center of the payload in the I-F ( $x_l, y_l, z_l$ ) are denoted by.

$$\begin{aligned} x_l &= x + l \sin \alpha \cos \beta \\ y_l &= y + l \sin \alpha \sin \beta \\ z_l &= z - l \cos \alpha \end{aligned} \quad (7)$$

The matrix  $J = J(\eta)$  is the inertia matrix and it is defined as follows.

$$J = \begin{bmatrix} I_\psi s_\theta^2 + I_\theta c_\theta^2 s_\phi^2 + I_\phi c_\theta^2 c_\phi^2 & c_\theta c_\phi s_\phi (I_\theta - I_\phi) & -I_\psi s_\theta \\ c_\theta c_\phi s_\phi (I_\theta - I_\phi) & I_\theta c_\phi^2 + I_\phi s_\phi^2 & 0 \\ -I_\psi s_\theta & 0 & I_\psi \end{bmatrix} \quad (8)$$

The short symbols  $s_\theta = \sin(\theta)$ ,  $c_\theta = \cos(\theta)$ . Also, the whole system potential energy represented by  $V(q)$ . It is equal to the sum of quadrotor potential energy and swinging load potential energy as follows:

$$V(q) = Mgz + m_l g z_l \quad (9)$$

Using (5), (6) and (9), the Lagrangian may be written as.

$$\begin{aligned} L &= \frac{1}{2} (M + m_l) (\dot{x}^2 + \dot{y}^2 + \dot{z}^2) + \frac{1}{2} (I_\psi s_\theta^2 + I_\theta c_\theta^2 s_\phi^2 + I_\phi c_\theta^2 c_\phi^2) \dot{\psi}^2 \\ &\quad + \frac{1}{2} (I_\theta c_\phi^2 + I_\phi s_\phi^2) \dot{\theta}^2 + \frac{1}{2} I_\psi \dot{\phi}^2 \\ &\quad + (I_\theta c_\theta c_\phi s_\phi - I_\phi c_\theta c_\phi s_\phi) \dot{\psi}^2 \dot{\theta}^2 - I_\psi s_\theta \dot{\psi}^2 \dot{\phi}^2 \\ &\quad + m_l l \dot{\beta} s_\alpha (c_\beta \dot{y} - s_\beta \dot{x}) + m_l l \dot{\alpha} c_\alpha (s_\beta \dot{y} + c_\beta \dot{x}) + \frac{1}{2} m_l l^2 \dot{\alpha}^2 \\ &\quad + \frac{1}{2} m_l l^2 s_\alpha^2 \dot{\beta}^2 + m_l l z s_\alpha \dot{\alpha} + \frac{1}{2} I (\dot{\alpha}^2 + \dot{\beta}^2) - Mgz - m_l g z_l \end{aligned} \quad (10)$$

By utilizing the Euler-Lagrange formulation, the dynamical model of the whole system is represented in the matrix form as follows.

$$M(q) \ddot{q} + C(q, \dot{q}) \dot{q} + G(q) = U \quad (11)$$

Where  $M(q) \in R^{8 \times 8}$  is the mass matrix,  $C(q, \dot{q}) \in R^{8 \times 8}$  is the Coriolis and centrifugal matrix,  $G(q) \in R^{8 \times 1}$  is the gravity matrix, and  $U \in R^{8 \times 1}$  is the generalized force in which  $U = b \times u$ .

These matrices are as follows.

$$M(q) = \begin{bmatrix} m_{11} & 0 & 0 & 0 & 0 & 0 & m_{17} & m_{18} \\ 0 & m_{22} & 0 & 0 & 0 & 0 & m_{27} & m_{28} \\ 0 & 0 & m_{33} & 0 & 0 & 0 & m_{37} & 0 \\ 0 & 0 & 0 & m_{44} & m_{45} & -I_{\psi} s_{\theta} & 0 & 0 \\ 0 & 0 & 0 & m_{54} & m_{55} & 0 & 0 & 0 \\ 0 & 0 & 0 & -I_{\psi} s_{\theta} & 0 & I_{\psi} & 0 & 0 \\ m_{71} & m_{72} & m_{73} & 0 & 0 & 0 & m_{77} & 0 \\ m_{81} & m_{82} & 0 & 0 & 0 & 0 & 0 & m_{88} \end{bmatrix}$$

Where  $m_{11} = m_{22} = m_{33} = M + m_l$ ,  $m_{17} = m_{71} = m_l \cos \alpha \cos \beta$ ,  $m_{18} = m_{18} = -m_l \sin \alpha \sin \beta$ ,  $m_{27} = m_{72} = m_l \cos \alpha \sin \beta$ ,  $m_{28} = m_{82} = m_l \sin \alpha \cos \beta$ ,  $m_{37} = m_{73} = m_l s_{\alpha}$ ,  $m_{44} = I_{\psi} s_{\theta}^2 + c_{\theta}^2 (I_{\theta} s_{\phi}^2 + I_{\phi} c_{\phi}^2)$ ,  $m_{45} = m_{54} = (I_{\theta} - I_{\phi}) (c_{\theta} s_{\phi} c_{\phi})$ ,  $m_{55} = I_{\theta} c_{\phi}^2 + I_{\phi} s_{\phi}^2$ ,  $m_{77} = m_l l^2 + I$  and  $m_{88} = m_l l^2 s_{\alpha}^2 + I$

(12)

$$c(q) = \begin{bmatrix} 0 & 0 & 0 & 0 & 0 & 0 & c_{17} & c_{18} \\ 0 & 0 & 0 & 0 & 0 & 0 & c_{27} & c_{28} \\ 0 & 0 & 0 & 0 & 0 & 0 & m_l l c_{\alpha} \dot{\alpha} & 0 \\ 0 & 0 & 0 & c_{44} & c_{45} & c_{46} & 0 & 0 \\ 0 & 0 & 0 & c_{54} & c_{55} & c_{56} & 0 & 0 \\ 0 & 0 & 0 & c_{64} & c_{65} & 0 & 0 & 0 \\ 0 & 0 & 0 & 0 & 0 & 0 & 0 & -m_l l^2 s_{\alpha} c_{\alpha} \dot{\beta} \\ 0 & 0 & 0 & 0 & 0 & 0 & m_l l^2 s_{\alpha} c_{\alpha} \dot{\beta} & m_l l^2 s_{\alpha} c_{\alpha} \dot{\alpha} \end{bmatrix}$$

Where  $c_{17} = -m_l l (c_{\alpha} s_{\beta} \dot{\beta} + s_{\alpha} c_{\beta} \dot{\alpha})$ ,  $c_{18} = -m_l l (c_{\alpha} s_{\beta} \dot{\alpha} + s_{\alpha} c_{\beta} \dot{\beta})$ ,  $c_{27} = m_l l (c_{\alpha} c_{\beta} \dot{\beta} - s_{\alpha} s_{\beta} \dot{\alpha})$ ,  $c_{28} = m_l l (c_{\alpha} c_{\beta} \dot{\alpha} - s_{\alpha} s_{\beta} \dot{\beta})$ ,  $c_{44} = I_{\psi} \dot{s}_{\theta} c_{\theta} - (I_{\theta} + I_{\phi}) (\dot{\theta} s_{\theta} c_{\theta} s_{\phi}^2) + (I_{\theta} - I_{\phi}) \dot{\phi} c_{\theta}^2 s_{\phi} c_{\phi}$ ,  $c_{45} = I_{\psi} \dot{\psi} s_{\theta} c_{\theta} - (I_{\theta} - I_{\phi}) (\dot{\theta} s_{\theta} c_{\theta} s_{\phi} + \dot{\phi} c_{\theta} s_{\phi}^2) - (I_{\theta} + I_{\phi}) (\dot{\psi} s_{\theta} c_{\theta} c_{\phi}^2 - \dot{\phi} c_{\theta} c_{\phi}^2)$ ,  $c_{46} = - (I_{\psi} \dot{\theta} c_{\theta} - (I_{\theta} - I_{\phi}) (\dot{\psi} s_{\theta} c_{\theta} c_{\phi}))$ ,  $c_{54} = \dot{\psi} s_{\theta} c_{\theta} (-I_{\psi} + I_{\theta} s_{\theta}^2 + I_{\phi} c_{\theta}^2)$ ,  $c_{55} = - (I_{\theta} - I_{\phi}) (\dot{\phi} s_{\theta} c_{\theta})$ ,  $c_{56} = I_{\psi} \dot{\psi} c_{\theta} + (I_{\theta} - I_{\phi}) (-\dot{\theta} s_{\theta} c_{\theta} + \dot{\psi} c_{\theta} c_{\phi}^2 - \dot{\psi} c_{\theta} s_{\phi}^2)$ ,  $c_{64} = - (I_{\theta} - I_{\phi}) (\dot{\psi} c_{\theta}^2 s_{\phi} c_{\phi})$  and  $c_{65} = -I_{\psi} \dot{\psi} c_{\theta} + (I_{\theta} - I_{\phi}) (\dot{\theta} s_{\theta} c_{\theta} + \dot{\psi} c_{\theta} s_{\phi}^2 - \dot{\psi} c_{\theta} c_{\phi}^2)$ .

(13)

$$G(q) = [0 \quad 0 \quad (M + m_l)g \quad 0 \quad 0 \quad 0 \quad m_l l g s_{\alpha} \quad 0]^T$$

$$b(q) = \begin{bmatrix} s_{\alpha} s_{\psi} + c_{\varphi} c_{\psi} s_{\theta} & 0 & 0 & 0 \\ c_{\varphi} s_{\theta} s_{\psi} - c_{\psi} s_{\varphi} & 0 & 0 & 0 \\ c_{\theta} c_{\varphi} & 0 & 0 & 0 \\ 0 & 1 & 0 & 0 \\ 0 & 0 & 1 & 0 \\ 0 & 0 & 0 & 1 \\ 0 & 0 & 0 & 0 \\ 0 & 0 & 0 & 0 \end{bmatrix}$$

$$\text{and } u = [u_1 \quad u_2 \quad u_3 \quad u_4]^T$$

By defining the state vector as.

$$X_1 = q, \quad \dot{X}_1 = X_2, \quad X = [X_1 \quad X_2]^T = [q \quad \dot{q}]^T \quad (14)$$

The Eq. (11) is expressed in state space form as.

$$\dot{X} = F(X, U) \quad (15)$$

In which  $F$  is defined in terms of  $Z \in R^{8 \times 8}$  and  $N \in R^{8 \times 1}$  as follows.

$$F = [F_1 \quad F_2]^T$$

$$F_1 = X_2, \quad F_2 = \dot{X}_2 = N(X_1, X_2) + Z(X_1)U \quad (16)$$

$$Z = M^{-1}, \quad N = -M^{-1}(C(X_1, X_2) + G(X_1))$$

### 3 Optimal Control Problem

The purpose of trajectory planning is to move the quadrotor from the initial configuration to the desired final configuration by controlling the angular velocity of rotors. Because of the high number of degrees of freedom and the complexity of the dynamical equations, solving the optimization problem in the general mode is a difficult task. Hence, an optimization model and an appropriate algorithm are defined to determine the optimal trajectory of the quadrotor. However, the presented method is easy and accurate to find suitable maneuvers for arbitrary initial and final states relevant to every considered cost function. In this part, the indirect solution to the optimal control problem is used for the off-line global trajectory planning of a quadrotor. If  $\bar{u}(t)$  is admissible control value in a period  $t \in [t_o \quad t_f]$ , The purpose of optimal control problem is to detect the amount of control  $u^*(t) \in \bar{U}$ , so that quadrotor in equation (15) minimizes the objective function  $J$ .

$$J(U, m_l) = \int_{t_o}^{t_f} L(X, U, m_l) dt = \frac{1}{2} \|X_1\|_{W_1}^2 + \frac{1}{2} \|X_2\|_{W_2}^2 + \frac{1}{2} \|U\|_R^2 \quad (17)$$

The integrand  $L(\cdot)$  is a smooth and differentiable function in the arguments.  $X(t)$ ,  $U(t)$  are the state space form of the generalized coordinate and the torque of the rotors, respectively.  $\|X\|_K^2 = X^T K X$  is the generalized squared norm.  $W_1$ ,  $W_2$ , and  $R$  denote the symmetric, positive definite  $(K \times K)$  matrices. The designer can decide on the relative importance among the control effort, angular position and velocity as well as load oscillation by changing the values of penalty matrices values  $W_1$ ,  $W_2$ , and  $R$ .

After forming the objective function, according to the indirect method, by introducing the co-state vector  $\lambda$ , the Hamiltonian function of the system is formed as:

$$H(X, U, \lambda, m_l, t) = L(X, U, m_l) + \lambda^T(t) F(X, U, m_l) \quad (18)$$



With respect to boundary conditions  $X(t_0) = X_0$ ,  $X(t_f) = X_f$  which show the positions and velocities of the system at starting point and ending point of maneuver and assuming a set of admissible inputs  $\bar{U} = \{U^- \leq U \leq U^+\}$ . Pontryagin's Minimum Principle then states the essential condition for a local minimum is that  $H$  be minimized with respect to  $\bar{U}$  for all  $t \in [t_0 \ t_f]$ . These conditions are equivalent to

$$\dot{X} = \frac{\partial H}{\partial \lambda} \quad \dot{\lambda} = -\frac{\partial H}{\partial X} \quad 0 = \frac{\partial H}{\partial U} \quad (19)$$

The optimal trajectory is then acquired by solving the 2n differential equations.

$$\dot{X}^*(t) = \frac{\partial H}{\partial \lambda}(X^*(t), U^*(t), \lambda^*(t), t) \quad (20)$$

$$\dot{\lambda}^*(t) = -\frac{\partial H}{\partial X}(X^*(t), U^*(t), \lambda^*(t), t) \quad (21)$$

$$H(X^*(t), U^*(t), \lambda^*(t), t) \leq H(X^*(t), \bar{U}(t), \lambda^*(t), t) \quad (22)$$

In which the symbol \* notes to the extremals of  $X(t)$ ,  $U(t)$ , and  $\lambda(t)$ .

The control values are confined with upper and lower bounds. The actuators that are usually employed for medium and small sizes quadrotors are the permanent magnet DC motor. The torque speed characteristic of D.C motors is represented as follow [22]:

$$U^+ = K_1 - K_2 X_2, \quad U^- = -K_1 - K_2 X_2 \\ K_1 = [\tau_{s1} \ \tau_{s2} \ \tau_{s3} \ \tau_{s4}]^T \quad K_2 = \text{diag} \left[ \frac{\tau_{s1} \ \tau_{s2} \ \tau_{s3} \ \tau_{s4}}{\omega_1 \ \omega_3 \ \omega_3 \ \omega_4} \right] \quad (23)$$

Where  $\tau_s$  is the stall torque (torque generated by the motor when fully "ON" but unable to move) and  $\omega_m$  is the maximum no-load angular velocity of the motor.

According to the description provided, Fig. 2 shows the schematic system architecture of the optimal control strategy. It comprises of two loops, namely, the main loop that produces the optimal signal " $U^*$ " and the other one is subsidiary loop that estimates the parameters " $X^*$ ", " $\lambda^*$ ". In the subsidiary loop, the block of the Quadrotor Dynamic Model represents the dynamic model of the system that is derived from the governing equations of the quadrotor. This block receives the desired trajectory and sends the ideal state of the model to the State Estimation. The state estimation block obtains the current state by comparing the state of the model and the data it receives from the Inertial Measurement Unit (IMU) sensor. Also, in the main loop, the block of Optimal Control calculates the optimal signal

by data it receives from IMU sensor and state estimation and gives it to the Quadrotor.

The set of optimality condition, the dynamic equations, and the boundary conditions establish a two-point boundary value problem (TPBVP) which is solvable by numerical techniques such as collocation, multiple shooting, and other similar methods. In this investigation, the `bvp4c` command in MATLAB software which is based on the collocation method is applied to solve. The method iterates on the initial values of the co-state until the ultimate boundary conditions are satisfied by the following favorable precision:

$$h(X(t_f), t_f) = \frac{1}{2} \|X_1(t_f) - X_{1f}\|_{w_p}^2 + \frac{1}{2} \|X_2(t_f) - X_{2f}\|_{w_v}^2 \leq \varepsilon \quad (24)$$

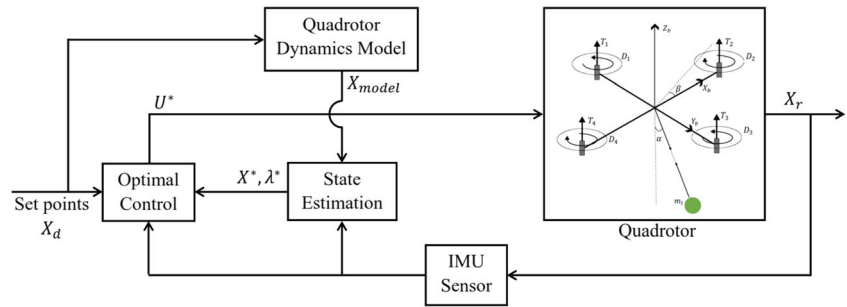
In this part, an appropriate algorithm is provided to calculate the maximum payload in Fig. 3.

As shown in Fig. 3. First, two points are selected at the workspace. Also, for long trajectories, a set of points can be given to the system. The proposed algorithm determines the optimal trajectory between two points sequentially. Then, the penalty matrices  $W_1$ ,  $W_2$ ,  $R$  are chosen. Also  $e$ ,  $n$ , which represent the precision at the estimation of maximum payload, and the number of iterations, respectively. The calculation process is based on the increase in the amount of payload from the minimum amount until the maximum payload is obtained. This algorithm consists of 2 loops. In the first loop index  $i$  increases the tip mass  $m_l$  until one point of one of the actuators torque reaches the upper or lower torque bounds. The upper and lower actuators torque range is equal to  $U^- \leq u \leq U^+$  and the favorable precision  $\varepsilon$  in TPBVP solution should be satisfied for the payload in every repetition. In the condition of carrying a payload more than  $m_{l \max}$  required a torque over than the admissible range of torque. Thereupon, the favorable precision  $\varepsilon$  could not be satisfied. In this situation, in the second loop index  $k$  decreases the amount of payload until the maximum payload for the supposed penalty matrices values is obtained with the precision  $\varepsilon$ .

## 4 Simulation Results

In this section, a simulation study is performed to confirm the effectiveness and accuracy of the proposed method for a quadrotor system with a swinging load for different objective functions. Simulations are undertaken for three cases. In the first case, the optimal path for the maximum payload capacity of the system is generated corresponding to defined penalty matrices. In the second case, the optimal path for the minimum oscillation of the swinging load is generated by changing the

**Fig. 2** Schematic system architecture



values of the penalty matrices. In the third case, the ratio of cable length to quadrotor length is studied in order to find optimal cable length to increase the maximum payload capacity and reduce the oscillation angles. Also, the effect of the ratio of load mass to quadrotor mass on the oscillation angles is studied.

### 4.1 First Case Study: Determining the Optimal Path for Maximum Payload

The linear external force is the entire thrust force of every four rotors. Hence, if the maximum thrust of each rotor is taken as

$T_{max} = 3 \text{ N}$ , the control inputs are limited to Eq. (25). According to the Eq. (4).

$$\begin{aligned} -3N &\leq u_1 \leq 12N \\ -6N &\leq u_2 \leq 6N \\ -6N &\leq u_3 \leq 6N \\ -6N &\leq u_4 \leq 6N \end{aligned} \quad (25)$$

The parameters associated with the quadrotor are shown in Table 1.

The problem is finding the most suitable path in which the quadrotor can carry the maximum possible payload. Therefore, the values of the penalty matrices are taken to be  $W_1 = W_2 = [0]$ ,  $R = \text{diag}(1)$ . Value of the favorable precision in the solution of TPBVP and the calculation of maximum payload are taken as  $\varepsilon = 0.001$  and  $e = 0.01$ , respectively. According to the proposed algorithm in Fig. 3,  $m_l$  increases from  $m_{l \min}$  up to  $m_{l \max}$  can be obtained. Therefore, the optimal trajectories can be found from the initial configuration  $X_0 = [1.5m, -2m, 2m, 0, 0, 0, 0, 0]$  at  $t_0 = 0$  to the desired final configuration  $X_f = [-1m, 2m, 2.5m, 0, 0, 0, 0, 0]$  at  $t_f$ . The initial and final velocities of the quadrotor system are zero.

As shown in Fig. 4, by increasing step by step amount of payload, the torque needed is increased and control input curves tend to their limits. Due to overcome the gravitational force, the first control input "u1" is more than the other ones and also, because of low-speed maneuvering, other control inputs are close to zero. Hence, when one point of the curve "u1" reaches to the specified limits, the maximum payload is obtained. The maximum payload proportional to these penalty matrices is obtained to be 0.3 kg.

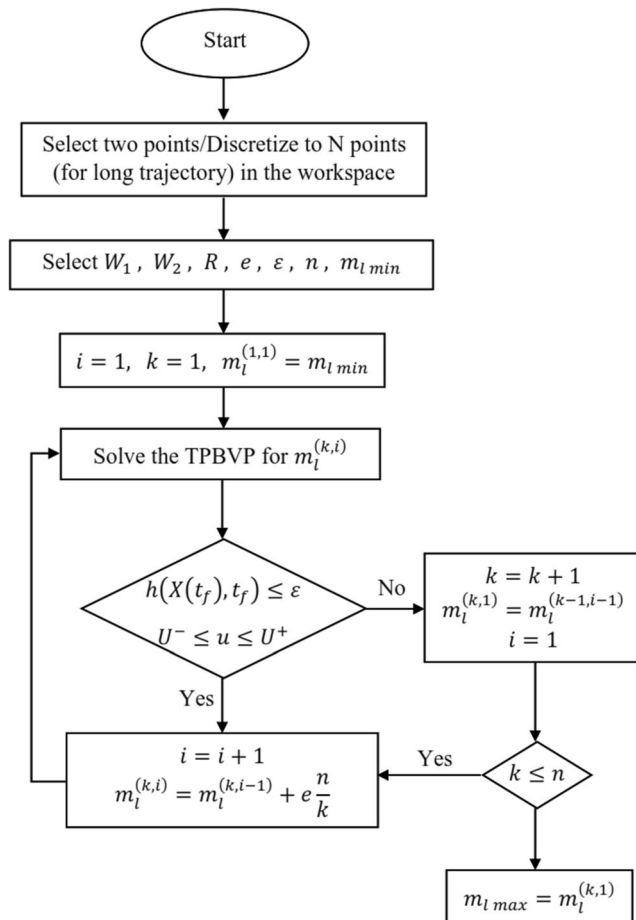


**Fig. 3** Maximum payload calculation algorithm

**Table 1** Physical parameters of the system

Parameter	Value
m (kg)	0.56
l (m)	0.242
r (m)	1
$I_l$ (kg. m <sup>2</sup> )	$m_l l^2$
$I_x = I_y$ (kg. m <sup>2</sup> )	6.178e-3
$I_z$ (kg. m <sup>2</sup> )	2.1e-3

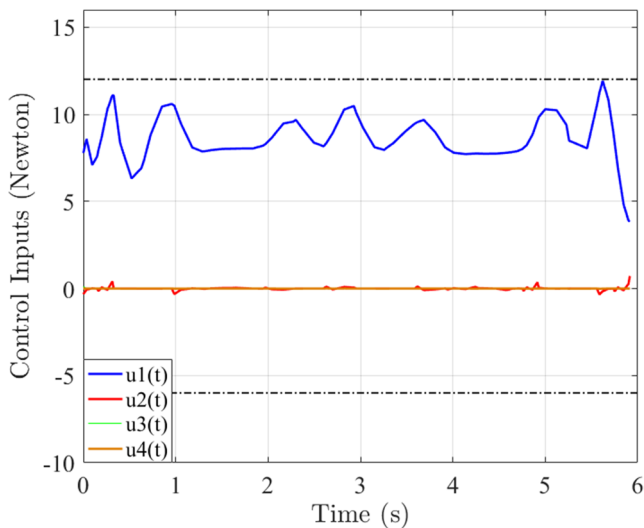


**Fig. 4** Optimal control inputs within upper and lower acceptable boundaries for maximum payload

The optimal trajectory planning of quadrotor with the maximum payload from an initial configuration to a final configuration in three-dimensional space is shown in Fig. 5. The values of oscillation angles ( $\alpha$ ,  $\beta$ ) of swinging load are displayed in Fig. 6. In Figs. 7 and 8 also, the position and attitude of the quadrotor relative to time are shown, respectively.

In order to validate the robustness of the proposed control strategy. A comparative simulation is performed to the observation of system behavior in an ideal environment and in a noisy environment like wind disturbance. For this purpose, an external disturbance with white Gaussian noise is applied to the system.

The results show in Fig. 9, the robustness of the proposed control strategy with respect to parameterized uncertainties and external disturbances.

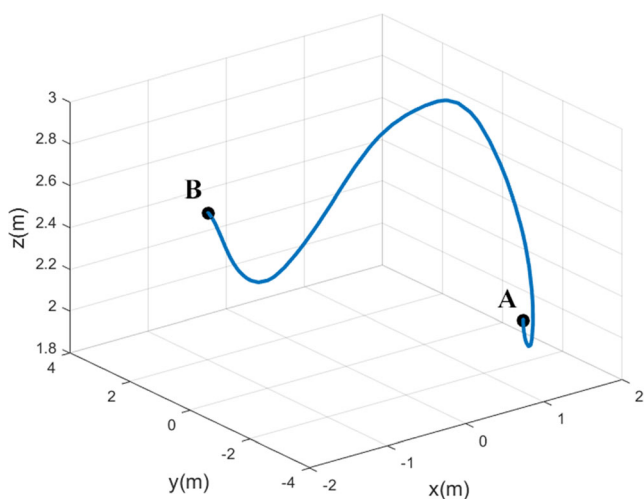


**Fig. 5** Optimal path for quadrotor between initial and final configuration with the maximum payload

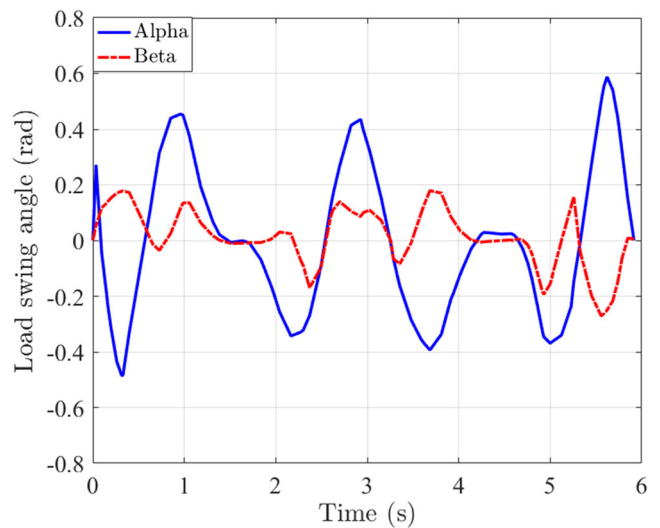


**Fig. 6** Load swing angle relative to time

Also, in order to verify the proposed solution, a simulation experiment is presented in Fig. 10 in which a set of points in a circular path given to the system. Initial position  $X_i = [0, 2, 1.6]$ . The proposed algorithm determines the optimal trajectory with maximum payload between given points sequentially. The robot rotates around origin of coordinates with radius 2 (m) and angle  $\frac{7\pi}{4}$  (rad) and finally arrives to the final position  $X_f = [-1.4, 1.4, 3]$ .

#### 4.2 Second Case Study: Determining the Optimal Path for Minimum Oscillation of the Swinging Load

As already mentioned, a quadrotor system with a cable-suspended load has a lot of degrees of freedom as well as, the effects of load mass and the moment of inertia arising from large oscillation angle can lead to quadrotor imbalance or even

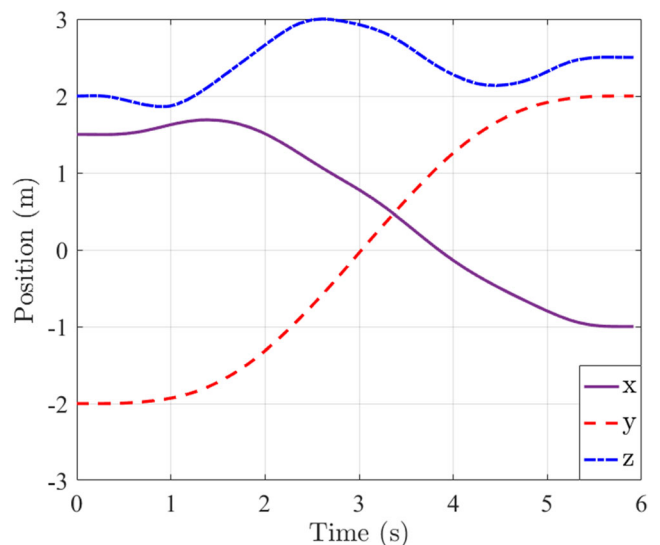


**Fig. 7** The position of quadrotor relative to time



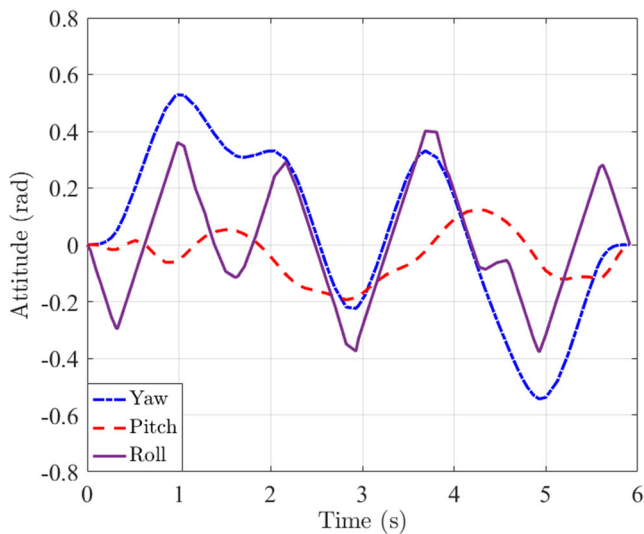


**Fig. 8** The attitude of quadrotor relative to time

overthrow. Therefore, in this section, the optimal trajectory for a quadrotor system with minimum swinging load's oscillation will be generated. In the next section, the optimal cable length to increase load capacity and reduce oscillation is determined

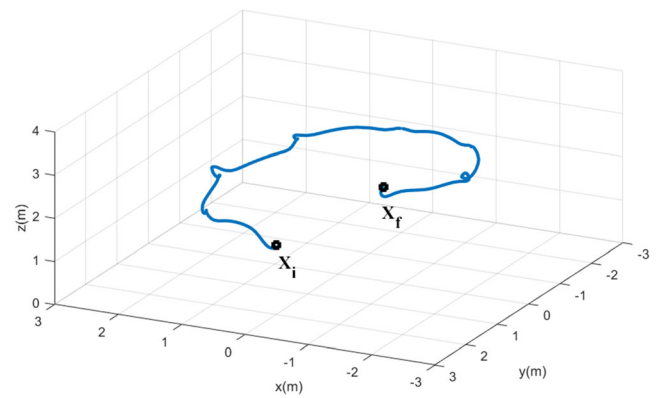


**Fig. 10** determined circular trajectory for the robot with maximum payload

and the effect of load mass on oscillation of swinging load is also investigated.

In the following, a path is simulated in which addition to carrying the maximum payload which was found in the previous section (0.3 kg), the quadrotor has the lowest oscillation of the swinging load and a more stable attitude. The values of penalty matrices are taken to be  $W_1 = W_2 = [1]$ ,  $R = \text{diag}(0.1)$ .

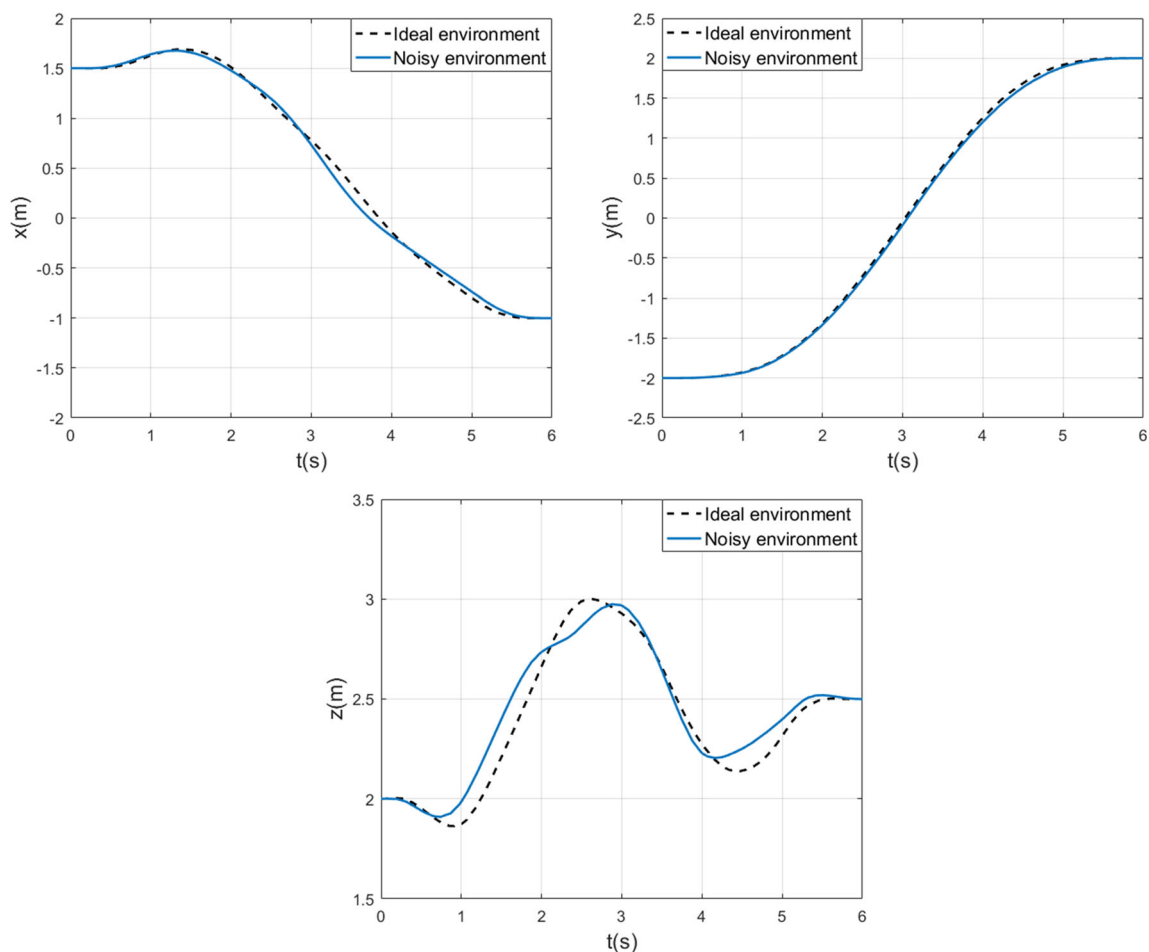


**Fig. 9** Comparative simulation to investigate system behavior in ideal and noisy environments

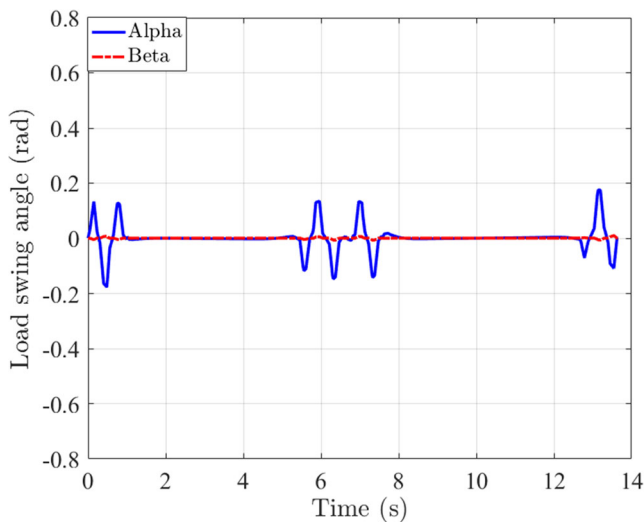


Fig. 11 Minimum oscillation of suspended load angles relative to time

This is important that the penalty matrix  $R$  decreased to “0.1”. it means that energy consumption has increased compared to the previous one. Also, for clarity of effectiveness of the proposed algorithm the flying time isn’t fix.

And the other conditions remain identical as the previous case study. The minimum oscillation angles relative to time are shown in Fig. 11. Also, the optimal path for the quadrotor with maximum payload and minimum oscillation angles is depicted in Fig. 12.

Fig. 13 shows the oscillation of Euler’s angles in minimum mode. In this case, the quadrotor maintains its sustainability and has a safer flight. As can be seen in Fig. 14, optimal control inputs are obtained within the specified range and should be applied as inputs to the quadrotor during optimal maneuvers. The fluctuations in the first control input “ $u_1$ ” are due to control and reducing oscillation of suspended load at

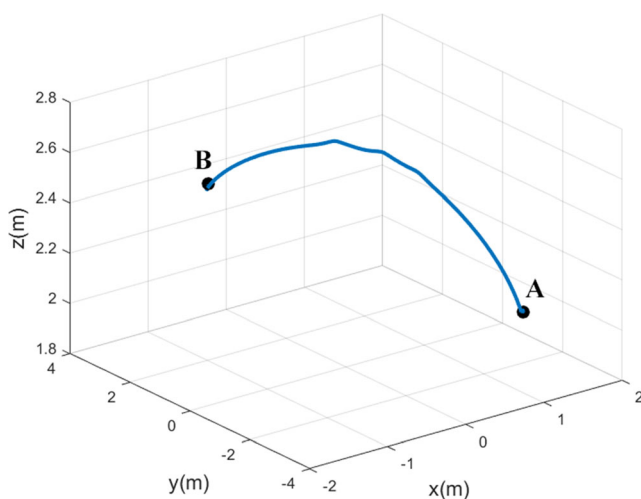


Fig. 12 Optimal path for quadrotor between initial and final configuration with minimum swing angles

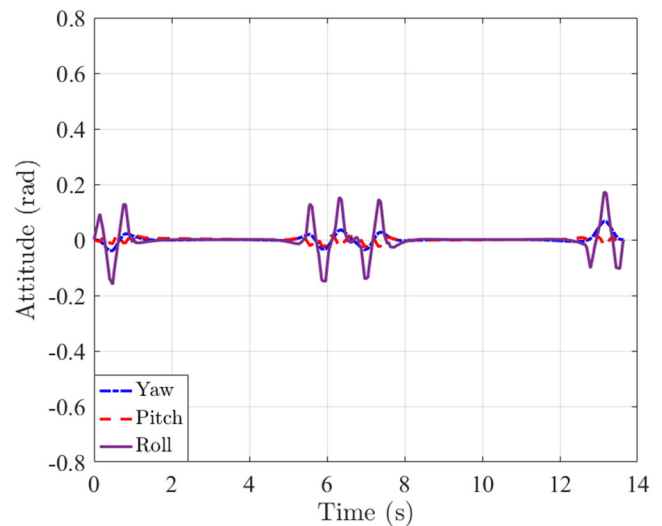


Fig. 13 Minimum oscillation of Euler angles relative to time

the start, peak and end of the maneuver. Also, Fig. 15 shows the position of quadrotor relative to time. In these conditions, the flight duration has increased to about 14 s.

#### 4.3 Third Case Study: Determine the Optimal Cable Length and Survey of the Effect of Load Mass on the Swinging load’s Oscillation

In this section, the effect of cable length relative to quadrotor length on the maximum payload capacity and maximum oscillation angle of the swinging load has been studied. The ratio of cable length to quadrotor length is denoted by  $\mu$ .

$$\mu = \frac{L(\text{cable})}{L(\text{quadrotor})} \quad (26)$$

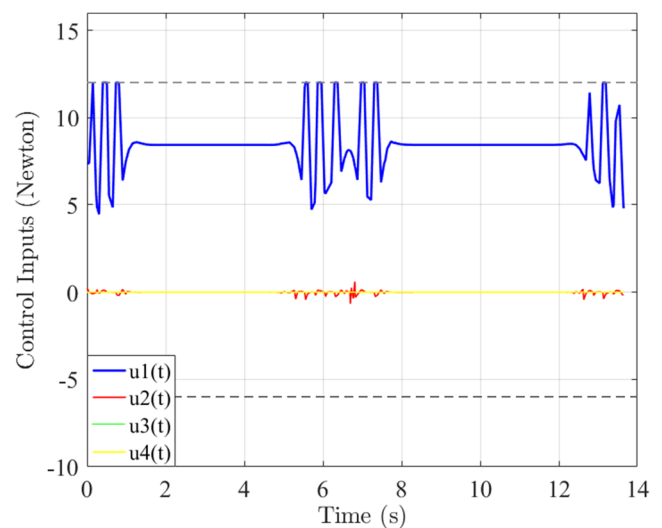


Fig. 14 Optimal control inputs within upper and lower acceptable boundaries for minimum oscillation of suspended load

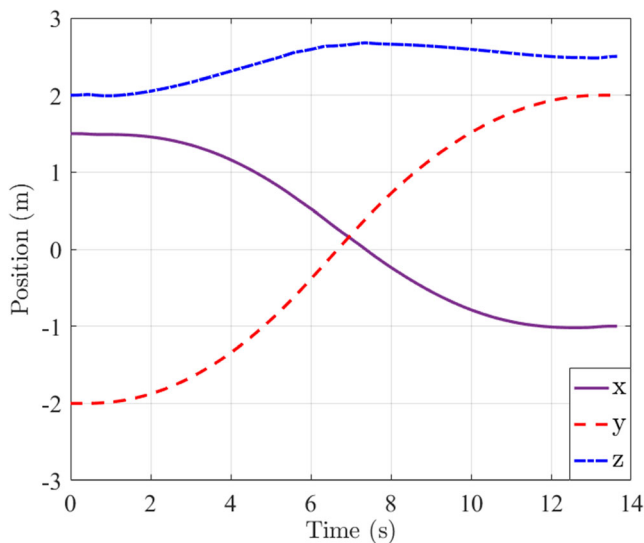


Fig. 15 Position of quadrotor relative to time

The values of penalty matrices are taken to be  $W_1 = W_2 = [1]$ ,  $R = \text{diag}(1)$  and the other conditions remain identical as the previous case study.

In Fig. 16, the x-axis represents the ratio of cable length to quadrotor length  $\mu$ , the y-axis represents the maximum oscillation angle of swinging load between  $\alpha$ ,  $\beta$  and the z-axis represents the maximum payload capacity of the quadrotor. As shown in the graph, by increasing the cable length relative to the quadrotor length, at point “P” maximum payload capacity increases to 0.34 (kg). While increasing further than this ratio causing decrease the maximum payload carrying capacity and generally, increase the load swing angles  $\alpha$ ,  $\beta$ . These are respectively shown in Figs. 17 and 18. At point P, for a quadrotor with a length of 0.242 (m), the cable length is equal to 1.4 (m) and the maximum oscillation angle of swinging load is equal to 0.6104 (radians).

By decreasing the cable length relative to the length of the quadrotor at point “Q” the minimum oscillation angle of

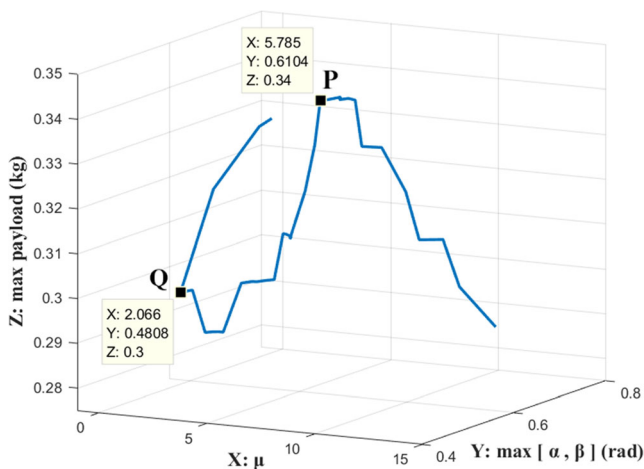


Fig. 16 The effect of cable length relative to quadrotor length on maximum payload and maximum oscillation angle of the swinging load

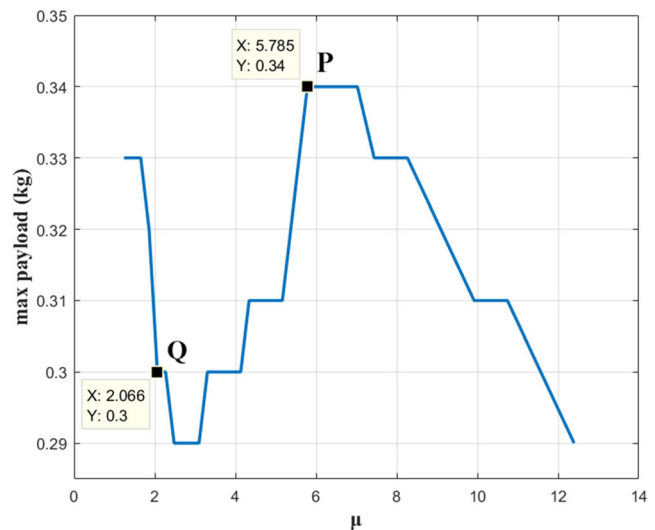


Fig. 17 The changes in the maximum payload value

swinging load is observed while the maximum payload is reduced to 0.3 (kg). At point Q, the cable length is equal to 0.5 (m) and the maximum oscillation angle of swinging load is equal to 0.4808 (radians). Decreasing further than this ratio causing increase the maximum payload carrying capacity as well as the maximum oscillation angle of swinging load eventually up to 0.7178 (rad) and 0.33 (kg), respectively. These are clearly shown in Figs. 17 and 18.

Figure 17 shows the maximum payload changes caused by increasing the ratio of  $\mu$  which is calculated with accuracy  $e = 0.01$ .

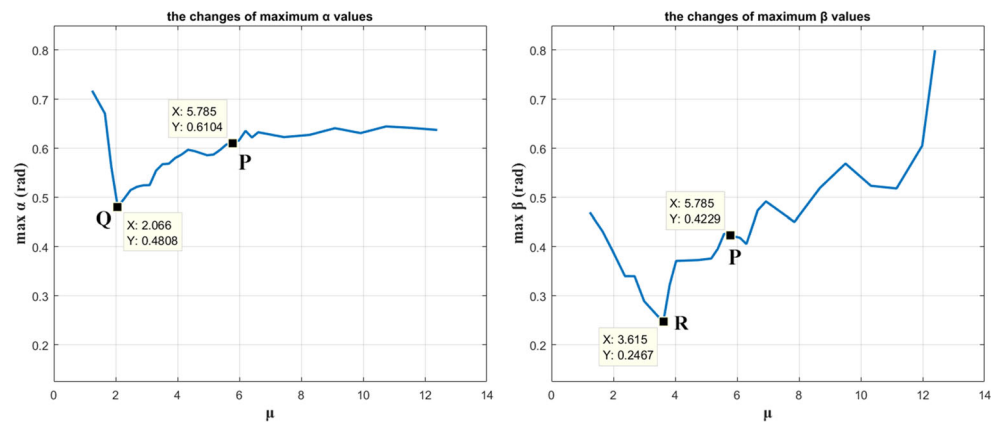
In Fig. 18, points Q and R denote the minimum value of the angles of  $\alpha$  and  $\beta$  respectively. But in this situation, due to the parameters and limits applied to the path, the  $\alpha$  angle has more values than  $\beta$ . Hence, it is relatively more important. According to the results obtained, for this quadrotor with the length of 0.242 (m), the cable length of 1.4 (m) is the most suitable length for carrying more payload and the cable length of 0.5 (m) is the most suitable length for least oscillation angle of the swinging load.

Oscillation of swinging load, in addition to possible damage to the load and disturb quadrotor balance condition, in some operations it is dangerous. Hence, in this part, the effect of load mass relative to the quadrotor mass on maximum oscillation angle of swinging load has been studied. The ratio of load mass to quadrotor mass is denoted by  $\nu$ .

$$\nu = \frac{m_l (\text{payload})}{M (\text{quadrotor})} \quad (27)$$

As shown in Fig. 19, assuming the cable length is equal to 1 m. By increasing the load mass relative to the quadrotor mass from 0.02 to 0.3 (kg), the maximum oscillation angle of swinging load is increased from 0.036 to 0.588 (rad). Consequently, selecting fewer payload causes reduce the

**Fig. 18** The changes in the maximum values of  $\alpha$  and  $\beta$  due to an increase of  $\mu$



maximum oscillation angle of swinging load. Finally, besides the calculated optimal cable length and calculated optimal paths. It's important to know about how to implement proposed method. Since the implementation of proposed method requires to deal with vector and matrix operations. Therefore, it is important to choose a suitable software library, hardware and various other. We will address this in the future.

## 5 Conclusions

Cargo transportation is one of the most important applications of quadrotor UAVs. A key feature needed for the application of these robots under complex conditions is the trajectory generator. Because of underactuated and nonlinear nature of the quadrotor dynamics as well as a large number of degrees of freedom and differential constraints, the trajectory planning problem is complicated. Hence, this paper presents a heuristic approach for optimal path planning which is based on the solution of optimal control problem from the class of the open

loop with an indirect method in the point-to-point maneuver. In this procedure, a perfect model of the nonlinear equation is used and all types of constraints are considered. The generalized Euler-Lagrange formulation was used to derive dynamic equations of a quadrotor system with a cable-suspended load. The model predicts the effect of the generated torques and thrust forces by the four propellers on the quadrotor motion. Hamiltonian function for an appropriate objective function was formed. According to the PMP, optimality essential conditions were acquired. Thus, the problem of determining the maximum payload or minimum oscillation angles converts to the standard form of a two-point boundary value problem which was solved by BVP4C command in MATLAB software. One advantage of the proposed method is the ability to solve a wide range of optimal maneuvers for arbitrary initial and final configurations relevant to every considered cost function. Finally, in order to prove the accuracy and importance of the suggested method, several simulations were performed for a quadrotor system with a cable-suspended load to optimal trajectory planning between two specified points with the different objective functions such as minimum effort and minimum swinging load's oscillation. The results indicate the effect of the suggested procedure on the performance improvement of quadrotor systems. Also, in this procedure, the designer can optimize the various objectives in proportion to their importance by changing the penalty matrices values and it yields to choose the best trajectories from the different paths.

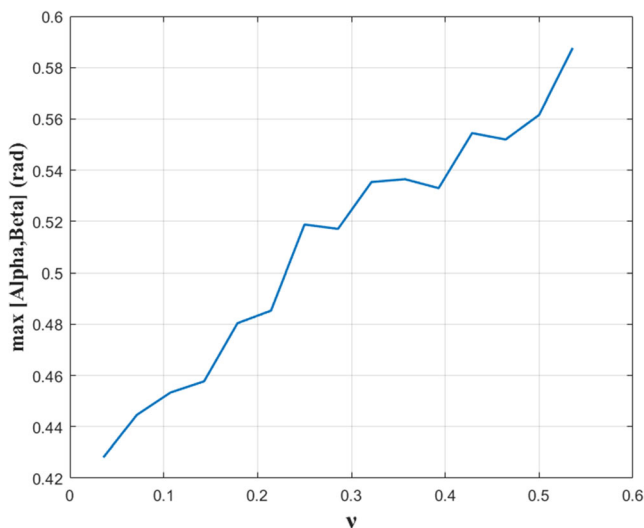


**Fig. 19** Effect of load mass relative to the mass of the quadrotor on maximum oscillation angle of the swinging load

## References

1. N. Sadati and A. Babazadeh: "A new hierarchical approach for optimal control of robot manipulators". In: Robotics, Automation and Mechatronics, 2004 IEEE Conference, pp.306–311 (2004)
2. Hehn, M., D'Andrea, R.: Real-time trajectory generation for quadcopters. IEEE Trans. Robot. **31**, 877–892 (2015)
3. T. Bresciani: "Modelling, Identification and Control of a Quadrotor Helicopter," MSc Theses, Department of automatic control. Lund Univ. (2008)

4. H. Fernando, A. De Silva, M. De Zoysa, K. Dilshan, and S. Munasinghe: "Modelling, simulation and implementation of a quadrotor UAV". In: Industrial and Information Systems (ICIIS), 2013 8th IEEE International Conference. pp. 207–212 (2013)
5. T. Luukkainen: "Modelling and control of quadcopter", *Indep Res Project Appl Math*, Espoo. **22**, 2011
6. Bousbaine, A., Wu, M.H., Poyi, G.T.: "Modelling and Simulation of a Quad-Rotor Helicopter," in *6th IET International Conference on Power Electronics, Machines and Drives (PEMD 2012)*, pp. 1–6. Bristol, UK (2012)
7. Mellinger, D., Michael, N., Kumar, V.: Trajectory generation and control for precise aggressive maneuvers with quadrotors. *Int J Robotics Research*. **31**, 664–674 (2012)
8. M. Hehn and R. D'Andrea: "A flying inverted pendulum". In: Robotics and Automation (ICRA), 2011 IEEE International Conference, pp. 763–770 2011
9. D. Mellinger and V. Kumar: "Minimum snap trajectory generation and control for quadrotors". In: Robotics and Automation (ICRA), 2011 IEEE International Conference, pp. 2520–2525 2011
10. M. Guerrero, D. Mercado, R. Lozano, and C. García: "Passivity based control for a quadrotor UAV transporting a cable-suspended payload with minimum swing". In: Decision and Control (CDC), 2015 IEEE 54th Annual Conference, pp. 6718–6723, 2015
11. Klausen, K., Fossen, T.I., Johansen, T.A.: Nonlinear control with swing damping of a multirotor UAV with suspended load. *J Intell Robotic Syst*. **88**, 379–394 (2017)
12. Navabi, M., Mirzaei, H.: Robust optimal adaptive trajectory tracking control of quadrotor helicopter. *Latin American J Solids Struct*. **14**, 1040–1063 (2017)
13. Shao, X., Liu, J., Cao, H., Shen, C., Wang, H.: Robust dynamic surface trajectory tracking control for a quadrotor UAV via extended state observer. *Int J Robust Nonlinear Control*. **28**, 2700–2719 (2018)
14. Shi, D., Wu, Z., Chou, W.: Harmonic extended state observer based anti-swing attitude control for Quadrotor with slung load. *Electronics*. **7**, 83 (2018)
15. Y. Bouktir, M. Haddad, and T. Chettibi: "Trajectory planning for a quadrotor helicopter," in *Control and Automation, 2008 16th Mediterranean Conference on*, 2008, pp. 1258–1263
16. I. D. Cowling, O. A. Yakimenko, J. F. Whidborne, and A. K. Cooke: "A prototype of an autonomous controller for a quadrotor UAV," In: Control Conference (ECC), 2007 European. 2007, pp. 4001–4008
17. Rosales, C., Gandolfo, D., Scaglia, G., Jordan, M., Carelli, R.: Trajectory tracking of a mini four-rotor helicopter in dynamic environments-a linear algebra approach. *Robotica*. **33**, 1628–1652 (2015)
18. Hehn, M., Ritz, R., D'Andrea, R.: Performance benchmarking of quadrotor systems using time-optimal control. *Auton. Robot*. **33**, 69–88 (2012)
19. Lai, L.-C., Yang, C.-C., Wu, C.-J.: Time-optimal control of a hovering quad-rotor helicopter. *J. Intell. Robot. Syst*. **45**, 115–135 (2006)
20. Ghariblu, H., Korayem, M.H.: Trajectory optimization of flexible mobile manipulators. *Robotica*. **24**, 333–335 (2006)
21. Wang, C.-Y., Timoszyk, W.K., Bobrow, J.E.: Payload maximization for open chained manipulators: finding weightlifting motions for a Puma 762 robot. *IEEE Trans. Robot. Autom.* **17**, 218–224 (2001)
22. Heidari, H., Haghpanahi, M., Korayem, M.H.: Payload maximization for Mobile flexible manipulators in an environment with obstacle. *J. Theor. Appl. Mech*. **53**, 911–923 (2015)
23. Jia, Z., Yu, J., Mei, Y., Chen, Y., Shen, Y., Ai, X.: Integral backstepping sliding mode control for quadrotor helicopter under external uncertain disturbances. *Aerosp. Sci. Technol*. **68**, 299–307 (2017)
24. Naidoo, Y., Stopforth, R., Bright, G.: Quad-rotor unmanned aerial vehicle helicopter modelling & control. *Int. J. Adv. Robot. Syst*. **8**, 45 (2011)
25. Benallegue, A., Mokhtari, A., Fridman, L.: High-order sliding-mode observer for a quadrotor UAV. *Int J Robust Nonlinear Control: IFAC-Affil J*. **18**, 427–440 (2008)

**Publisher's Note** Springer Nature remains neutral with regard to jurisdictional claims in published maps and institutional affiliations.

**Danial Hashemi** received his B.Sc. in 2018 in mechanical engineering at Malayer university. He is currently (2020) an M.Sc student at Arak university in Arak. His research interests include Optimization, Energy conversion/storage, UAV path planning.

**Hamidreza Heidari** is an assistant professor at the Malayer University in Malayer. In 2011, he has received his PhD from the IUST University. His research interests include Dynamics, Nonlinear Vibration, Flexible Manipulators, and energy harvesting.